

A bright source for infrared microspectroscopy: synchrotron radiation

Paul Dumas^a and Mark J. Tobin^b

^aLURE, centre Universitaire Paris Sud, BP 34, F-91898 Orsay Cédex, France

^bCCLRC Daresbury Laboratories, Warrington, Cheshire WA4 4AD, UK

Introduction

Infrared spectroscopy (IR) is one of the techniques for investigating matter that has a very long history of use in both research and applied sciences.

In the early 1980s Fourier transform infrared (FT-IR) spectrometers were coupled with a microscope,¹ since when the success of IR microanalysis has increased rapidly. Nowadays, IR-microscopy has gained wide acceptance in various scientific communities as a qualitative microanalytical tool for identifying the chemical make-up of isolated contaminants or characterising localised areas of much larger samples. The FT-IR microscopes now commercially available include many of the features of research-grade optical microscopes: polarisation, Nomarski Difference Interference Contrast, fluorescence, as well as sophisticated software for generating chemical images and analysis. Perhaps one indicator of the growing acceptance is the recognition by biologists of the importance of IR microspectroscopy as a potential tool for biondiagnosis.

Present day FT-IR spectrometers and microscopes are well matched and deliver high performance. However, signal-to-noise ratio (S/N) requirements often limit the smallest practical spot size to ~20 μm diameter. This limitation is not the consequence of diffraction or aberration in the optical system of the IR microscope, but rather due to the low intrinsic brightness (defined as the photon flux or power emitted per source area and solid angle) of the thermal infrared source.

The diagnostic potential of IR-microspectrometric data strongly depends on the quality of the spectra acquired.

As with many of today's analytical techniques, FT-IR spectroscopy is increasingly moving into imaging technology enabled by detector developments that were originally available only to the military, for example, for missile guidance technology. These detectors have improved dramatically during the past decade to a point that mercury-cadmium-telluride IR focal plane array detectors are now routinely used with infrared spectroscopy.

Higher signal-to-noise values are often considered as a fundamental measure for achieving a better detection and spectral quality. For most infrared detectors, the Noise Equivalent Power (NEP) is proportional to the square root of their active area.² Small area detectors are now routinely employed in IR microscopy. The quality of the spectra depends also on the infrared source. The commonly employed source is a blackbody heated to ~1400–2000 K. To increase further the IR microspectroscopy capability, brighter sources in the IR region are required.

For thermal sources, one has little control over the brightness apart from raising the temperature or changing the emissivity of the photon source.

A particle, such as an electron, emits synchrotron radiation when accelerated or (decelerated). The radiation is emitted along the direction of motion of the particles. A number of synchrotron accelerator facilities exist around the world specifically to provide an intense source of radiation. They have been exploited, for spectroscopy, in the VUV, far-UV and soft X-ray regions. Synchrotron radiation has been used successfully in both the mid-IR and far-IR regions for about ten years, and has an equivalent blackbody temperature in excess of 10,000 K! It is particularly

attractive for IR microspectroscopy, as exemplified in this article.

IR micro-spectroscopy

Synchrotron radiation: a bright source of infrared photons

Electron storage rings (or synchrotrons) use magnetic fields to bend electrons into a closed orbit. Synchrotron radiation is produced at each of the bending magnets. Infrared radiation is generated by electrons travelling at relativistic velocities, either inside a curved path through a constant magnetic field (bending magnet radiation)³ or by longitudinal acceleration or deceleration when leaving or entering a magnetic section (edge radiation).⁴ The emitted radiation spans an extremely broad spectral range, extending from the X-ray to the very far-infrared region.

The effective synchrotron source size is quite small, and can be on the order of ~100 μm . Furthermore, the light is emitted into a narrow range of angles.

The intensity distribution, for a particular wavelength, is dependent on the mode of emission, and has to be considered carefully, in order to optimise the extraction geometry and to couple efficiently all collected photons into the microscope.

This can be illustrated by considering the intensity profile of the beam at two characteristic wavelengths, 10 and 100 μm , and for a storage ring operating at an energy of 2.75 GeV, see Figure 1(a, b). In Figure 1, two extraction geometries have been considered

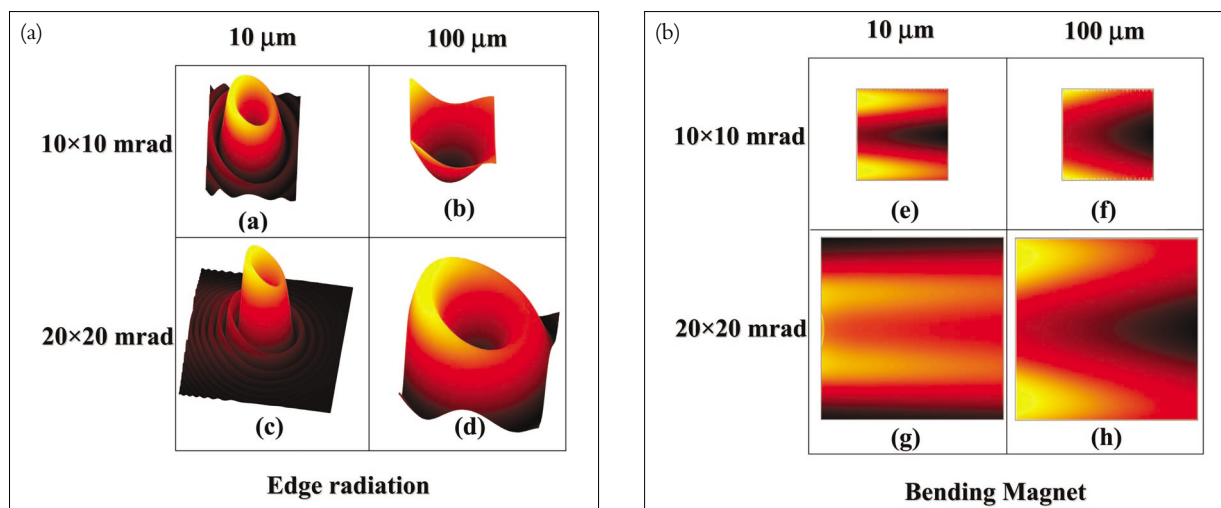


Figure 1. Calculated intensity profile for infrared emission at 10 μm and 100 μm , either from an edge radiation or a bending magnet radiation source (see text). The calculations have been carried out using the SRW code (O. Chubar and P. Elleaume) using the following parameters: electron energy = 2.75 GeV, electron current = 500 mA, magnetic field = 1.56 T, straight section length = 6 m, distance to point source = 1.5 m. Profiles have been calculated for two extraction geometries (horizontal \times vertical opening angles): 10 \times 10 and 20 \times 20 mrad. Colour code: Minimum = black, Maximum yellow. (For convenience, the profiles calculated for the bending magnet are shown in 2D displays.) This allows the operator to define parameters accurately for an optimum collection of infrared photons.

(opening angle: horizontal \times vertical): 10 \times 10 mrad and 20 \times 20 mrad. Clearly, the intensity of the emitted source is not distributed uniformly. For edge radiation, rings of maximum emission are produced, with increasing size for longer wavelengths. At 2.75 GeV (recent third generation synchrotron facilities have energy in the 2–3 GeV range), a 10 \times 10 mrad (e.g. 1.5 \times 1.5 cm^2 aperture positioned at 1.5 m from the source point) would be appropriate to collect most of the infrared photons at and below 10 μm . However, the far-infrared wavelength region will not be optimally collected [Figure 1(a) b]: for such a purpose, an aperture of 20 \times 20 mrad is preferable [Figure 1(a) d], but may affect the properties of the stored electron beam. These engineering issues are carefully considered in synchrotron facilities. An edge radiation source is radially polarised. For the constant field emission (bending magnet), the emission is distributed longitudinally, but is a minimum at the centre. Clearly, the collection is not yet optimised at 10 \times 10 mrad for a 10 μm wavelength [Figure 1(b) e], while a 20 \times 20 mrad aperture is appropriate for such a wavelength [Figure 1(b) g]. It would be necessary to increase the collection angles to collect, efficiently, the long wavelength radiation at 100 μm . It is important to note that by enlarging the horizontal aperture (they are usually rectangular in existing synchrotron IR beamlines) more photons can be collected. Such sources are highly polarised (along the longitudinal section).

The two types of synchrotron IR sources, edge radiation and bending magnet radiation, have equivalent flux and brightness. Depending upon engineering constraints of the particular synchrotron, one or the other is chosen. The synchrotron source has a brightness advantage about between two and three orders of magnitude compared to a blackbody source. At this point, it is particularly important to note that the brightness advantage does not mean that the synchrotron produces more power, but simply that the emitted photons can be coupled more effectively into an instrument such as a microscope. In spite of the increased infrared throughput of synchrotron microscopes, no induced damage has ever been detected, even on fragile biological samples.⁵

Another feature of synchrotron light is that it is pulsed, i.e. the electrons do not form a continuous distribution around the orbit, but instead they travel in “bunches”. Depending upon the storage ring, these bunches have lengths on the order of 1–10 cm, and this results in pulses of light on a sub-nanosecond time-scale, with which time-resolved studies can be undertaken.

Infrared microscopy with a Synchrotron source

FT-IR microscopes are available commercially from a number of instrument manufacturers worldwide. Very few modifications are needed in order to adapt a commercial instrument for use with a synchrotron infrared source.

The synchrotron beam can be efficiently collimated and is directed into the interferometer, which modulates the infrared light, and then is directed towards the IR microscope. Since the synchrotron source produces high throughput at small aperture sizes, the diffraction limit is achieved when the microscope’s apertures define a region with dimensions equal to the wavelength of interest. However, the use of a confocal optical arrangement leads to ~30% improvement in the spatial resolution, in agreement with diffraction theory.⁶

Some applications

Several synchrotron infrared microscopy beamlines are operating around the world, and several others are under construction or planned. Applications are multidisciplinary, and the number continues to increase as these beamlines become accessible to an increasing number of users. High spatial resolution, excellent spectral quality (signal-to-noise), and fast data acquisition are the essential features of the technique.

Polymer films studies

It is well known that vibrational microscopy is a powerful tool for characterising polymeric materials, providing both compositional and structural information. Most new polymeric materials are multiphase systems. They include homopolymers and copoly-

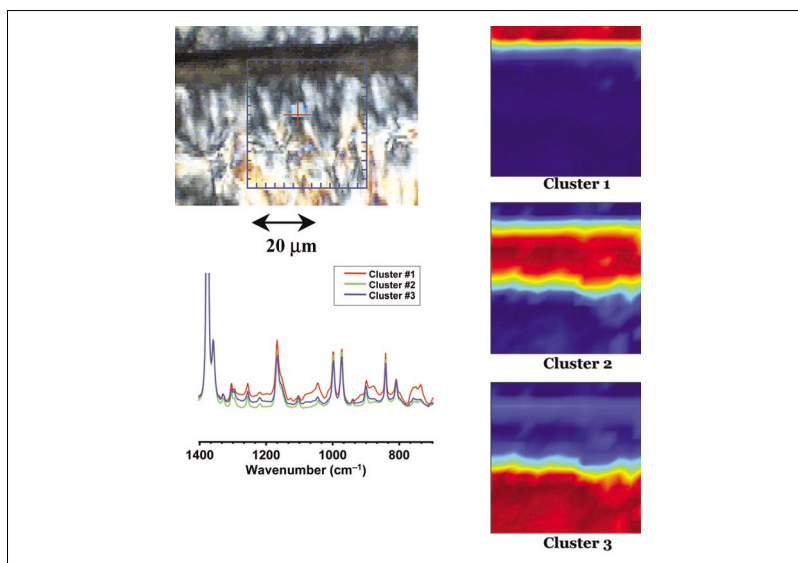


Figure 2. Infrared imaging of various polymorphic forms in a LCP fibre-reinforced iPP film where the fibre has been sheared at the isothermal crystallisation temperature. The optical image displays, within the blue square, the mapped area, with marked steps of 3 µm. From the cluster analysis of the spectra recorded, fuzzy-C means-clustering images have been generated, and each of the image clusters corresponds to different crystalline morphologies. The characteristic spectra of each cluster are also displayed, and subtle differences in spectra can be seen.

mers, polymer blends and composite materials, in which the physical and mechanical properties of the system are governed by the relative amounts of each component and/or their morphology (crystalline or amorphous), and their intrinsic properties. However, the type, size and distribution of the different domains in these materials, and the relationship or interaction between the different phases are also fundamental. In this respect, in addition to the obvious differences in the chemical structure of, for example, two polymers in a blend, these materials can present different types of heterogeneity: compositional, structural and morphological.

G. Ellis *et al.* have studied the polymorphism of isotactic polypropylene (iPP), using synchrotron infrared microscopy.⁷ In Figure 2 an example is shown which corresponds to a LCP (Liquid Crystalline Polymer) fibre-reinforced iPP film where the fibre has been sheared at the isothermal crystallisation temperature. Different crystalline habits can be observed in the visible image, and infrared spectra were obtained using a $3 \times 3 \mu\text{m}$ aperture over the area indicated. The spectroscopic identification of the different types of crystalline morphology is described elsewhere.⁷ However, in this case in order to differentiate between the various regions of the iPP film a statistical treatment of the spectra was undertaken by hierarchical cluster imaging using Cytospec software

(see <http://www.cytospec.com/ftir.html>). High S/N spectra were obtained even with the very small aperture. For a more optimum classification the first-derivative of each spectra was analysed over the $700\text{--}1350 \text{ cm}^{-1}$ region. Subtle differences were observed in the characteristic first-derivative spectra, and from these three clearly distinguishable features could be located in the hierarchical cluster images of the sampled area, which could be associated with different crystalline morphologies.

Human tissues investigations

IR spectroscopy is being employed increasingly in the study of biomedical conditions, where it has been shown to be capable of detecting subtle biochemical changes within tissues. The coupling of a microscope to a Fourier transform infrared spectrometer, complemented by the use of a synchrotron source has brought the potential to examine tissues at cellular and sub-cellular resolution.

The applicability of micro-spectroscopy, and hence imaging, in particular to biological and pathological problems relies on the information being obtained at high lateral spatial resolution. Spectroscopic imaging provides diagnostic information in a visual form, a prospect appealing to physicians and biologists. Image methods can provide potentially far more information to non-specialists than their non-imaging

counterparts. However, the analysis and diagnostic potential of IR imaging strongly depends on the quality of the spectra acquired. Clearly, a parameter such as the signal-to-noise ratio, strongly affects the image quality.

Hereafter, we illustrate how high spectral quality obtained at diffraction-limited spot size sheds new light into the biochemical composition and protein secondary structure of human tissues: in this case, hair.

Human hair sections have been studied intensively using synchrotron infrared microspectroscopy.⁸ They are $50\text{--}100 \mu\text{m}$ in diameter and their cross-section reveals three major identifiable regions. The medulla is the centre-most portion of the hair. It is $5\text{--}10 \mu\text{m}$ in thickness and composed of loosely packed, keratinised cells that distribute moisture and nutrients to the hair strand. The medulla can be either continuous or discontinuous along the hair length, and often it is completely absent. The cortex makes up the bulk of a hair fibre and determines the strength of a hair. It is $45\text{--}90 \mu\text{m}$ in diameter and composed of long embedded cortical cells. It also contains the hair pigment, melanin. The outermost layer of a hair strand is the cuticle, which is less than $5 \mu\text{m}$ in thickness. It is a dense layer of flat, keratinised cells, which protects the hair fibre. Infrared spectra were recorded across hair fibres with an aperture size of $3 \times 3 \mu\text{m}^2$.

The chemical images of the lipids (height of peak at 2920 cm^{-1}), displayed in Figure 3(a), show that lipids are predominantly located inside the outer cuticle layer, as well as inside the medulla (orange and red regions). The high quality of the recorded spectra has allowed subtle difference in the peak position and lineshape of the stretch modes of CH_2 to be observed between lipids located in the medulla or in the cuticle. Fuzzy-C means-clustering images have been generated in the $2800\text{--}3000 \text{ cm}^{-1}$ region, and associated images of the two main classes of CH_x stretch modes are shown in Figures 3(b) and 3(c), which reveal the different nature of the lipids in this two regions. These differences can be related to the relative chain lengths (CH_2/CH_3 ratio) of the prevalent lipids in each region.

IR spectroscopy can also reveal the different composition of the protein secondary structures. For hair sections, the Amide I band contour is different between spectra recorded from inside the cortex and from inside the cuticle, see Figure 3(e). The red spectrum has been recorded inside the cuticle, with an aperture of $3 \times 3 \mu\text{m}^2$. Clearly, the peak position exhibits a downward wavenumber shift, which indicates a higher relative concentration of β sheet to α

helix inside the cuticle. This relative concentration is shown in Figure 3(d).

Synchrotron infrared microscopy appears to be extremely well suited to the study of hair biochemical composition, and its variation with age, ethnic origin, sex etc., as well as for studying the interaction of external agents (for example, cosmetics) on hair composition and structure, and is the subject of several current investigations.

Single cell studies

Using synchrotron infrared microscopy, Jamin *et al.* were the first to demonstrate that the chemical components of single living cells, e.g. proteins, lipids, and nucleic acids, can be imaged with high signal-to-noise at a diffraction-limited spatial resolution.⁹ This work was pursued further by the extended study of programmed cell death, i.e. apoptosis, using a combination of fluorescence microscopy and synchrotron infrared microscopy.¹⁰

Detailing the bio-composition and protein secondary structures inside one single cell is a subject of paramount importance, in order to understand the changes of the cell cycle, as well as any abnormality that would ultimately lead

to a disease.

To illustrate the sub-cellular capability studies of synchrotron infrared microscopy, we have studied the behaviour of single HL60 cells during differentiation. HL60 cells are often studied as an attractive model for differentiation, and are used specifically for human myeloid cell differentiation. Among several agents used for differentiation, phorbol myristate acetate (PMA) induces HL60 cells to differentiate into mature monocytes/macrophages *in vitro*.

Figure 4 illustrates the main observations. Figure 4(a) shows the optical image of one HL60 cell before inducing the differentiation process. Chemical imaging of the lipid profile has been generated using the peak height at 2920 cm^{-1} [Figure 4(b)]. They are clearly distributed around the nucleus.

After 48 hours of differentiation induction time, a clear change in the Amide I lineshape is observed [Figure 4(c)]. It is suggested that following PMA treatment, the α -helix content, in differentiated cell membrane protein, increases. These changes in the membrane protein secondary structures are probably related to the mode of interac-

tion with the inducing agent. By using a statistical analysis in the Amide I and Amide II band frequency region ($1485\text{--}1710\text{ cm}^{-1}$) of the high S/N spectra obtained with a $3 \times 3\text{ }\mu\text{m}^2$ aperture, it is possible to separate out the different relative composition of the protein secondary structure, inside the nucleus and in the cytoplasm. Figure 4(d) shows the two cluster images and the average spectrum of each.

Only the use of a synchrotron source can produce such high contrast chemical images inside individual cells.

Future and perspectives

It is clear that synchrotron radiation provides a high brightness infrared source, which is being exploited successfully in microspectroscopy for high signal-to-noise spectra and for fast data acquisition, because of the readily achievable diffraction-limited spatial resolution. Several infrared microscopes are now implemented at synchrotron facilities around the world, although many applications are still in their infancy. An attractive feature of the synchro-

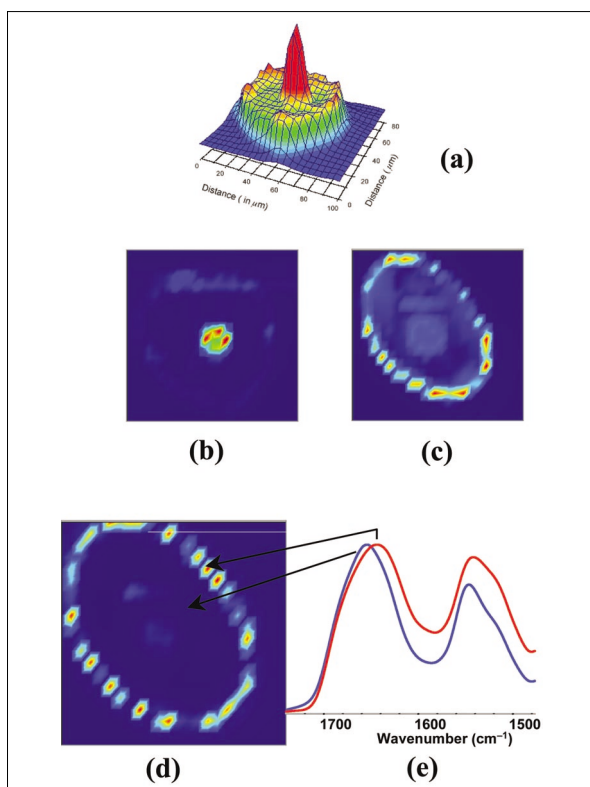


Figure 3. (a) Chemical image of lipids (peak height at 2920 cm^{-1}) across a human hair section. The IR map has been recorded with a $23 \times 3\ \mu\text{m}^2$ aperture. Using hierarchical cluster imaging, two types of lipids are recognised, and located either in the cuticle (b) or in the medulla (c). The amide I lineshape across the hair section is not homogeneous, and downward (wavenumber) displacement of the maximum is observed inside the cuticle. The image of the β sheet/ α helix ratio is displayed in (d) while the corresponding Amide I bands are shown in (e).

tron environment is the capability of achieving complementary characterisation using other available synchrotron-based microanalytical tools. Among them, X-ray microscopy is one of the best-suited complementary approaches to infrared microscopy.

Several improvements are now being proposed for synchrotron infrared microscopy. Nowadays, focal plane arrays detectors are being implemented in microscopes that use a globar source, and the performance of these detectors has not yet been exploited with a synchrotron source. Clearly, the size of the detector array has to be adapted to match the projected size of the synchrotron beam, in order to keep the brightness advantage of this source. These small detector arrays might well be available soon, and will allow faster acquisition data, and a slightly improved lateral resolution using point-spread function (PSF) deconvolution.

Interesting new attempts have been initiated with a synchrotron infrared source in order to extend measurements to below the diffraction limit¹¹ by

employing PhotoThermal IR Micro-Spectroscopy (PTMS), see Figure 5. In this technique, an AFM-based thermal probe is used as the infrared absorption sensor, and promising results have already been obtained.

All together, the bright infrared source provided by synchrotron radiation has a tremendous future, in microscopy and near-field microscopy, and such facilities are available to experimenters who are invited to contact the various synchrotron infrared beamline representatives. There are currently four operating beamlines in Europe (Daresbury, UK; ANKA, Germany; BessyII, Germany and LURE, France) and several others are under construction and will be available soon (Maxlab, Sweden; SLS, Switzerland; Elettra, Italy; ESRF, France; SOLEIL, France; Diamond, UK).

It is important to note that applications of synchrotron infrared spec-

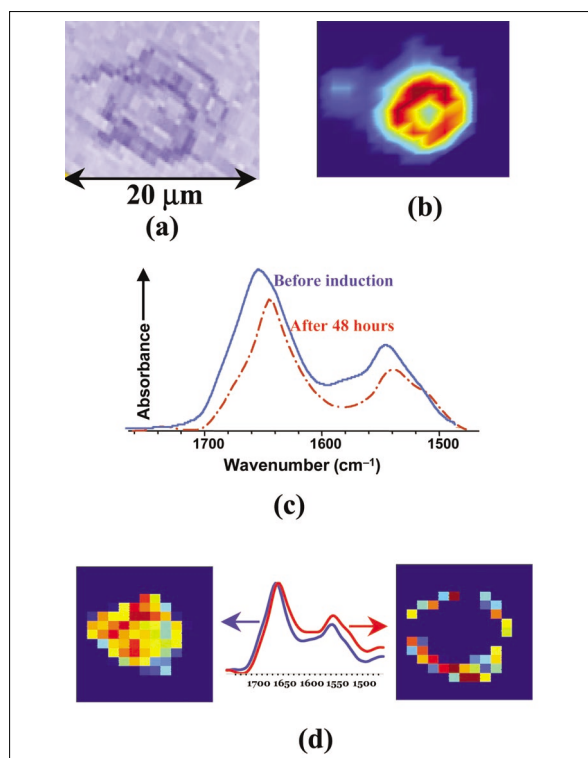


Figure 4. (a) Visible image of a single HL60 cell, of about $18\ \mu\text{m}$ diameter. (b) Chemical image of the lipids based on peak height at 2920 cm^{-1} , across the single cell shown in (a) and before differentiation induction. (c) Amide I and II frequency range for cell before and after 48 hours of differentiation induction, recorded with an aperture of $3 \times 3\ \mu\text{m}^2$. One can note the narrower lineshape of the Amide I band at 1655 cm^{-1} after differentiation induction. (d) An hierarchical cluster analysis, followed by fuzzy C-means clustering on a cell after differentiation reveals two slightly different protein secondary structure, inside the nucleus and in the cytoplasm. Average spectra of these two clusters are also displayed. All IR spectra have been recorded with a $3 \times 3\ \mu\text{m}^2$ aperture.

trosopy are not restricted to microscopy but also exhibit a tremendous prospect in other fields, such as far-infrared spectroscopy, time-resolved spectroscopy and two-colour experiments.

Acknowledgements

The authors wish to thank G.P. Williams, G.L. Carr, L.M. Miller, G.A. Ellis, H. Pollock, A. Hammiche and M.A. Chesters for their long-term collaboration and support, as well as for their very fruitful discussions.

References

1. A.J. Sommer, in *Handbook of Vibrational Spectroscopy*, Ed by J.M. Chalmers and P.R. Griffiths. John Wiley and Sons, Chichester, pp. 1369–1385 (2002).
2. E. Theocharous and J.R. Birch, in *Handbook of Vibrational Spectroscopy*,

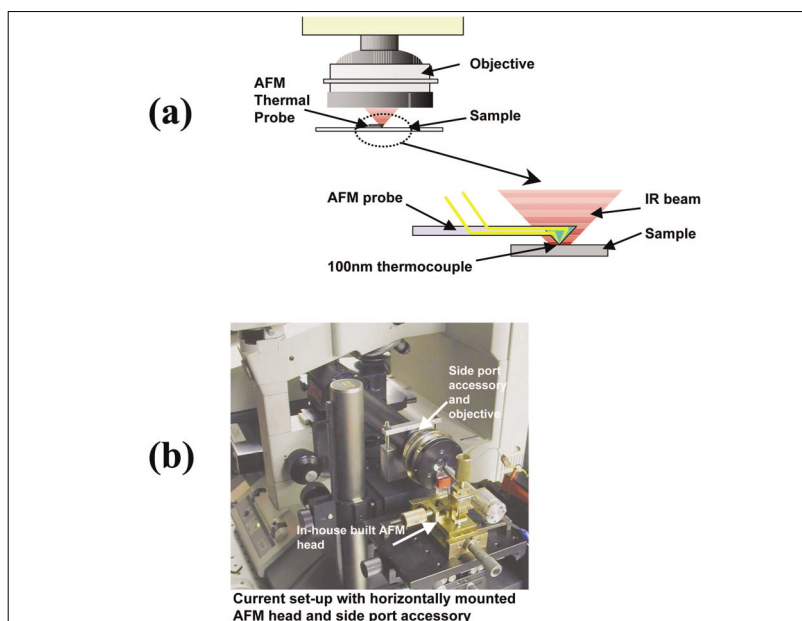


Figure 5. (a) PhotoThermal IR Micro-Spectroscopy. A microthermal probe, based on an atomic force microscope (AFM) cantilever tip is placed under the infrared microscope objective at the focus of the synchrotron light. Though the infrared light covers an area defined by the diffraction limit, the probe can potentially sense thermal absorptions from much smaller regions. By modulating the light, the output from the sensor can be used to generate an absorbance spectrum. (b) The scanning probe instrument is coupled to the infrared beamline at the SRS, Daresbury, using a side-port accessory.

Ed by J.M. Chalmers and P.R. Griffiths. John Wiley and Sons, Chichester, pp. 349–367 (2002).

3. W.D. Duncan and G.P. Williams, *Appl. Opt.* **22**, 2914 (1983).
4. R.A. Bosch, *Nucl. Instrum. Meth. Phys. Res. A* **386**, 525 (1997).
5. M.C. Martin, N.M. Tsvetkova, J.H. Crowe and W.R. McKinney, *Appl. Spectrosc.* **55**, 111–113 (2001).
6. G.L. Carr, *Rev. Sci. Instr.* **72**, 1–7 (2001).
7. G. Ellis, C. Marco and M.A. Gomez, *J. Macromol. Sci. - Phys.*, in press.
8. P. Dumas and L.M. Miller, *Vib. Spectrosc.*, in press.
9. N. Jamin, P. Dumas, J. Moncuit, W.-H. Fridman, J.L. Teillaud, G.L. Carr and G.P. Williams, *Proc. Natl. Acad. Sci. USA* **95**, 4837–4840 (1998).
10. L. Miller, P. Dumas, N. Jamin, J.L. Teillaud, J. Miklossi and L. Forro, *Rev. Sci. Instrum.* **73**, 1357–1360 (2002).
11. L. Bozec, A. Hammiche, M.J. Tobin, J.M. Chalmers, N.J. Everall and H.M. Pollock, *Meas. Sci. Technol.* **13**, 1217–1222 (2002).